World Academy of Science, Engineering and Technology
International Journal of Biotechnology and Bioengineering
Vol:6, No:7, 2012

Synchrotron X-ray based Investigation of Fe and Zn Atoms in Tissue Samples at Different Growth Stages

Sunil Dehipawala, Todd Holden, E. Cheung, Robert Regan, P. Schneider, G. Tremberger Jr, D. Lieberman, T. Cheung

***Abstract*—**The zinc and iron environments in different growth stages have been studied with EXAFS and XANES with Brookhaven Synchrotron Light Source. Tissue samples included meat, organ, vegetable, leaf, and yeast. The project studied the EXAFS and XANES of tissue samples using Zn and Fe K-edges. Duck embryo samples show that brain and intestine would contain shorter EXFAS determined Zn-N/O bond; as with the cases of fresh yeast versus reconstituted live yeast and green leaf versus yellow leaf. The XANES Fourier transform characteristic-length would be useful as a functionality index for selected types of tissue samples in various physical states. The extension to the development of functional synchrotron imaging for tissue engineering application based on spectroscopic technique is discussed.

***Keywords*—**EXAFS, Fourier Transform, metalloproteins, XANES

I. Introduction

ZINC and iron are important in metalloproteins that are involved in biological pathways with zinc metalloprotein being also implicated in neuro pathways [1]. Synchrotron X-ray based absorption spectroscopic technique has been used by various researchers to investigate the local environments of iron and zinc in metalloproteins [2]. It was reported that Fe-O and Fe-S have EXAFS bond lengths of 182 pm and 224 pm respectively in cytochrome 450 using the Advanced Photon Source at Argonne National Lab, USA [3]. They also listed the range of other reported Fe-O EXAFS bond lengths with a span from 164 to 193 pm, Fe-N EXAFS bond lengths with a span from 199 to 203 pm, Fe-S EXAFS bond lengths with a span from 221 to 248pm in Fe metalloproteins. Other synchrotron X-ray based spectroscopy investigations include the study of the efficiency of Rubisco, arguably the most abundance protein on Earth [4]. Although X-ray based technique has been well accepted for bond length determination, radiation damage was reported to be responsible for the gradual increase of Fe(IV)-O bond length from 173 pm to 190 pm in peroxidase ferryl intermediate involved in the metalloenzyme pathway [5]. The observed difference would be consistent with the iron-oxygen bond being a double bond at 173 pm and single bond at 190 pm as the high-intensity synchrotron x-ray sources could induce rapid reduction of metal centers, particularly high-potential metal centers such as Fe(IV) [6].

Sunil Dehipawala, Todd Holden, E. Cheung, Robert Regan, G. Tremberger Jr, D. Lieberman, and T. Cheung are with Physics Department Queensborough Community College, City University of New York (CUNY-QCC). Contact email: gtremberger@qcc.cuny.edu

P. Schneider is with Biology Department CUNY-QCC.

Recently the chemical form of Zn in the leaf tissue samples has been reported using Zn K-edge EXAFS spectroscopy at European Synchrotron Radiation Facility, France [7]. It was reported that Zn-O and Zn-C interatomic distances in the studied leaf samples span the range of 203 to 207 pm and 292 to 298pm respectively. Zn metalloprotein pathways are important in growth processes and it is expected that tissue samples at different growth stage would carry different zinc environment information. Fe metalloprotein pathways are important in metabolism and the Fe environment information would vary in different growth related metabolic pathways.

The zinc and iron environments in different growth stages have been studied with EXAFS and XANES with Brookhaven Synchrotron Light Source. The results of EXAFS and XANES tissue samples of meat, organ, vegetable, leaf, and yeast are presented.

II. Materials and Methods

The EXAFS and XANES data were collected at beamline X10C of National Synchrotron Light Source at Brookhaven national Laboratory. Rhodium coated cylindrical mirror is used to focus the beam on the sample. A double crystal Si(220) mono-chromator was used for energy selection. Ion chambers were used to measure beam intensity before the hutch, I0 (before sample), ant transmission intensity. A 7-element Si drift detector was used to measure fluorescence intensity. Piezoelectric driver using A/C feedback system locks the beam. Beam size on the sample was 10 mm x 2 mm. Beamline and data collection was controlled by microvax II computer running on VMS. The tissue samples were obtained from consumer sources, the calibration samples (Zn and Fe foils, Fe2O3, zinc oxalate, and ZnS) used for calibration were purchased from Sigma Aldrich. The data analysis was done with EXAFSPAK and WIN-XAS packages.

III. Results And Discussion

A typical EXAFS scan of a duck embryo tissue sample and its Fourier transform are shown in Figures 1 and 2 respectively. The results of tissue samples from a duck embryo are listed below in Table I.

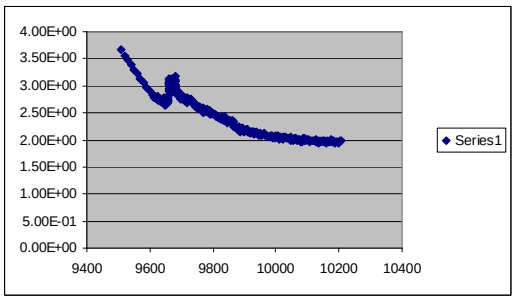

Fig. 1 The Zn EXFAS data of duck embryo thigh sample. The x-axis energy scale is in eV

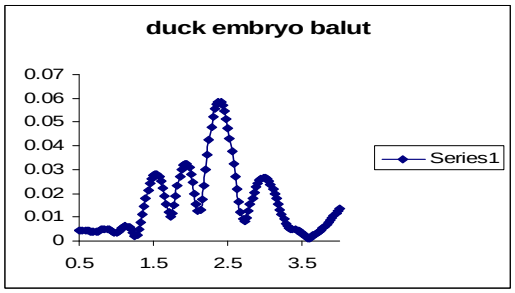

Fig. 2 The Fourier transform of duck embryo (balut) thigh k-cubed-weighted Zn EXAFS of Figure 1. The x-axis is in Angstrom (100 pm)

The first peak in the Fourier transform k-cubed weighted EXAFS data was ascribed to Zn-O or Zn-N contribution since N/O and S have different scattering amplitudes, the first-shell analysis can usually discriminate between the presence of N/O or S atoms [8].

TABLE I
SUMMARY OF DUCK EMBRYO TISSUE SAMPLE DATA

Animal	Tissue	Fourier Transform First Peak
Duck	thigh	237.4
	stomach	222.4
	liver	217.4
	heart	187.4
	intestine	157.2
	brain	142.4

A coarse separation of the duck embryo data into two groups would suggest that the brain and intestine samples have short Zn-N/O bond lengths as compared to the other studied samples. Furthermore continuous scan of a brain sample suggested the Zn-N/O bond length would increase by about 7 pm after 2 hours, perhaps related to some form of radiation damage.

The results of regular chicken tissue samples are listed below in Table II. A typical EXAFS scan of chicken tissue sample and its Fourier transform are shown in Figures 3 and 4 respectively.

TABLE II
SUMMARY OF CHICKEN TISSUE SAMPLE DATA

Animal	Tissue	Fourier Transform First Peak pm
Chicken	breast	234.9
	drumstick	217.4
	neck1	237.4
	neck2	247.1
	liver1	222.4
	liver2	214.9
	breast	234.9

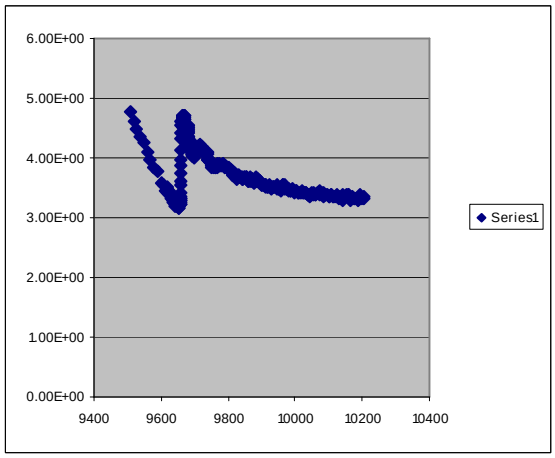

Fig. 3 The Zn EXFAS data of chicken breast sample. The x-axis energy scale is in eV

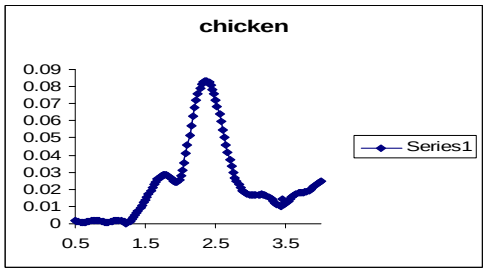

Fig. 4 The Fourier transform of chicken breast k-cubed--weighted Zn EXAFS of Figure 3. The x-axis is in Angstrom (100 pm)

The chicken tissue sample data suggests a sample variation of about 15 pm.

The results of yeast samples (baking yeast) are listed below in Table III. A typical EXAFS scan of yeast sample and its Fourier transform are shown in Figures 5 and 6 respectively.

TABLE III
SUMMARY OF YEAST SAMPLE DATA

Yeast	Sample Type	Fourier Transform First Peak pm
	fresh yeast	215
	reconstituted yeast	237

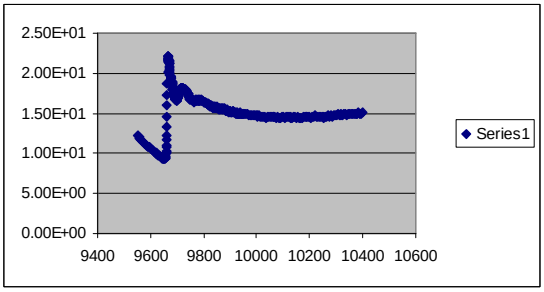

Fig. 5 The Zn EXFAS data of fresh yeast sample. The x-axis energy scale is in eV

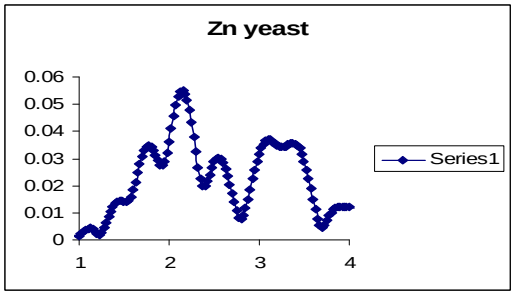

Fig. 6 The Fourier transform of fresh yeast k-cubed--weighted Zn EXAFS of Figure 3. The x-axis is in Angstrom (100 pm)

The fresh yeast EXAFS data suggests that shorter Zn-N/O bond length could be associated with efficacy, knowing that the reconstituted yeast from dry powder package passed the sugar growing test after the X-ray bombardment. This would suggest that the chicken drumstick (Table II) zinc metalloproteins carry higher efficacy, not to mention that the shortest Zn-N/O distance was observed in the embryo brain samples (Table I). Fresh green kale leaf sample data also suggest a shorter Zn-N/O bond length of 237pm as compared to yellow kale sample of 302pm. Protein folding models that treat all zinc motif as 220-pm first neighbor distance would be applicable to analyze such data for the modeling of the protein unfolding in decaying samples [9]. Future EXAFS studies may be able to confirm whether Zn-N/O bond length can serve as a functionality biomarker in tissue samples. The radiation damage could be avoided by using fast pulse source EXAFS [10] or short XANES scans. The project is interested in developing a bond length associated functionality biomarker with reference to EXAFS-Fourier methodology; the standard XANES analysis method of using a linear combination of XANES standard spectra would not be effective. In fact the actual bond length information for Fe-O has been extracted by the Fourier transform of the Fe K-edge XANES first shell data (k = [0.2625* (E − 7092.7)^1/2], that is, 3.9 to 5.8 A^{-1}) using model fitting in inorganic samples [11]. The Zn K-edge XANES data embedded in the EXAFS data revealed that Fourier transform is an acceptable method for obtaining a characteristic length (char-length) for comparison purpose. The XANES char-length resolution would be different than that of the EXAFS bond length data because the XANES spectra would contain information from Zn-N/O, and Zn-C, Zn-S bonds. In the event that the Zn XANES spectra up to 9800eV have major Zn-N/O contribution, correlation of Zn XANES Fourier transform char-length and EXAFS bond length was observed. For example, the XANES char-length for the duck embryo brain sample would be about 122 pm and the thigh would be 174 pm; with zinc oxalate sample at 160 pm (EXAFS bond length 200pm). An adjusted R-square value would be 0.95 N =3. A tissue sample with relatively less Zn-S bond would be most suitable for XANES Fourier analysis. In other words, the Zn-S (233 pm) in Cys2His2-like or Cys4-like zinc finger motif in Transcription Initiation Factor IIB would have contribution to the Zn-N/O XANES energy range in a tissue sample [12].

Similar procedures were carried out for the study of the Fe EXAFS and XANES data. The EXAFS data of a Spanish tissue sample is shown in Figure 7 and its Fourier Transform is shown in Figure 8.

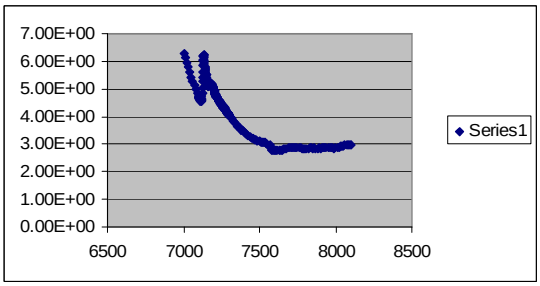

Fig. 7 The Fe EXFAS data of spinach tissue sample. The x-axis energy scale is in eV

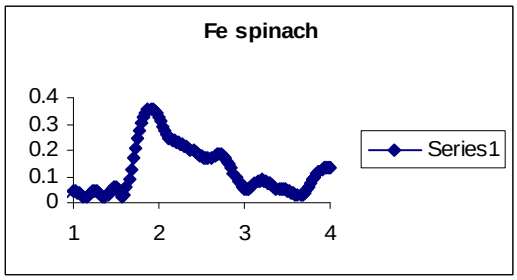

Fig. 8 The Fourier transform of spinach k-cubed--weighted Fe EXAFS of Figure 7. The x-axis is in Angstrom (100 pm)

The determined first neighbor was about 190 pm of Fe-N/O. The above-noise level peak at 220pm could be coming from Fe-S. Interestingly the Zn EXAFS spinach data result (Figure 9) also exhibits two peaks in its Fourier Transform (Figure 10).

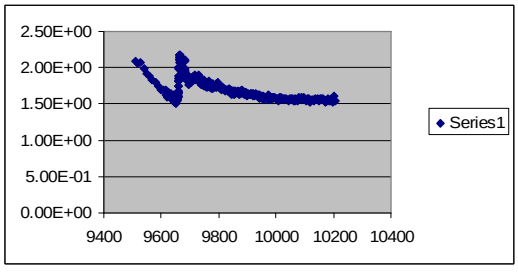

Fig. 9 The Zn EXFAS data of Figure-7 spinach sample. The x-axis energy scale is in eV

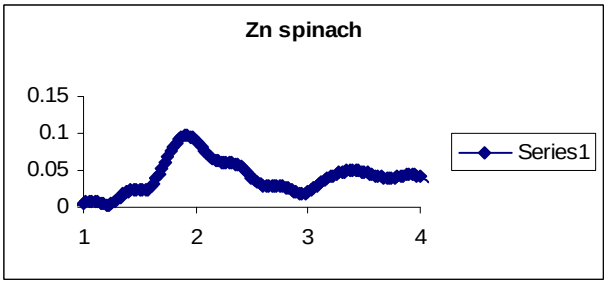

Fig. 10 The Fourier transform of spinach k-cubed--weighted Zn EXAFS of Figure7 the x-axis is in Angstrom (100 pm)

The determined first neighbor distance was about 195 pm of Zn-N/O. The above noise level peak at 240pm could be a Zn-S signature. .

The Fe XANES Fourier transform shows that cooked calf liver tissue sample has longer char-length as compared to raw calf liver tissue sample by about 60 pm.

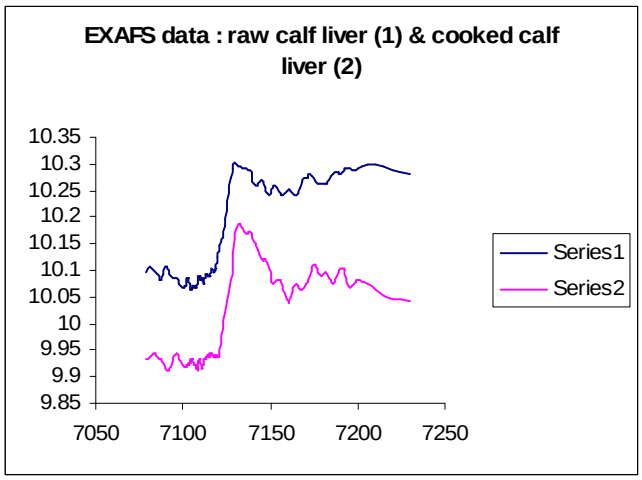

Fig. 11 The Fe XANES data of cooked calf liver sample (lower) and raw calf liver sample (upper). The x-axis energy scale is in eV

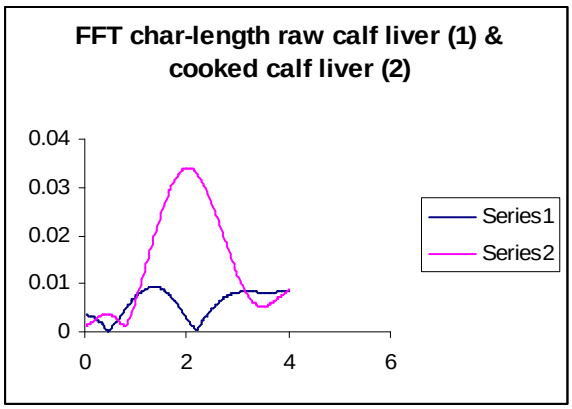

Fig. 12 The XANES Fourier transform of calf liver data (upper curve: cooked and raw lower curve: raw). The x-axis is in Angstrom (100 pm)

The XANES Fourier transform char-length could serve as a functionality index for selected type of tissue samples in various physical states. Future studies would be needed to develop the XANES Fourier transform char-length as a functionality index, for example, in pathological tissue sample imaging, genetic engineered tissue imaging, etc. The proposed automated black-box approach for biological EXAFS data analysis would be welcomed [13]. The microbial metalloproteomics prediction [14] and high throughput X-ray absorption data with Brookhaven X3B beamline on expressed microbial metalloproteins [15] would offer valuable guidance to the development of a functional synchrotron imaging for biotechnological applications based on spectroscopic technique.

IV. Conclusion

The project studied the EXAFS and XANES of tissue samples using Zn and Fe K-edges. Embryo samples show that brain and intestine would contain shorter EXFAS determined Zn-N/O bond; as with the case of fresh yeast versus reconstituted live yeast and green leaf versus yellow leaf. The XANES Fourier transform char-length would be useful as a functionality index for selected types of tissue samples in various physical states. Future studies could include the correlation study of EXAFS determined bond length with XANES Fourier transform characteristic length; and the use of the EXAFS technique to track metalloprotein folding mechanism in genetic engineered tissue samples.

Acknowledgment

Use of the National Synchrotron Light Source, Brookhaven National Laboratory, was supported by the U.S. Department of Energy, Office of Science, Office of Basic Energy Sciences, under Contract No. DE-AC02-98CH10886. R.R. thanks NSF-REU for the summer stipend. E.C. thanks the hospitality of QCC Physics Dept. The project was partially supported by several CUNY grants.

References

[1] Shi W, Chance MR. (2011) Metalloproteomics: forward and reverse approaches in metalloprotein structural and functional characterization Curr Opin Chem Biol. Feb;15(1):144-8.

[2] Ascone I & Strange R. (2009) Biological X-ray absorption spectroscopy and metalloproteomics. J Synchrotron Radiat. 2009 May;16(Pt 3):413-21.

[3] Newcomb M, Halgrimson JA, Horner JH, Wasinger EC, Chen LX, Sligar SG. (2008) X-ray absorption spectroscopic characterization of a cytochrome P450 compound II derivative. Proc Natl Acad Sci U S A. Jun 17;105(24):8179-84.

[4] Liu C, Hong FS, Tao Y, Liu T, Xie YN, Xu JH, Li ZR (2011). The mechanism of the molecular interaction between cerium (III) and ribulose-1,5-bisphosphate carboxylase/oxygenase (Rubisco). Biol Trace Elem Res. Nov;143(2):1110-20. Epub 2010 Oct 30.

[5] Meharenna, Y.T.; Doukov, T.; Li, H.; Soltis, S.M.; Poulos, T.L. "Crystallographic and single-crystal spectral analysis of the peroxidase ferryl intermediate," (2010) Biochemistry 49, 2984-2986.

[6] Corbett, M. C., Latimer, M. J., Poulos, T. L., Sevrioukova, I. F., Hodgson, K. O., and Hedman, B. (2007) Photoreduction of the active site of the metalloprotein putidaredoxin by synchrotron radiation. Acta Crystallogr D Biol Crystallogr 63, 951-960.

[7] Sarret G, Willems G, Isaure MP, Marcus MA, Fakra SC, Frérot H, Pairis S, Geoffroy N, Manceau A, Saumitou-Laprade P. (2009) Zinc distribution and speciation in Arabidopsis halleri x Arabidopsis lyrata progenies presenting various zinc accumulation capacities. New Phytol. Nov;184(3):581-95.

[8] Giachini L, Veronesi G, Francia F, Venturoli G, Boscherini F. (2010) Synergic approach to XAFS analysis for the identification of most probable binding motifs for mononuclear zinc sites in metalloproteins. J Synchrotron Radiat. Jan;17(1):41-52.
[9] Wang C, Vernon R, Lange O, Tyka M, Baker D. (2010) Prediction of structures of zinc-binding proteins through explicit modeling of metal coordination geometry. Protein Sci. Mar;19(3):494-506.
[10] Chen J, Zhang H, Tomov IV, Ding X, Rentzepis PM. (2008) Photochemistry and electron-transfer mechanism of transition metal oxalato complexes excited in the charge transfer band. Proc Natl Acad Sci U S A. Oct 7;105(40):15235-40.
[11] Bugaev L, Farges F, Rusakova E, Sokolenko A, Latokha Y, Avakyan L. (2005) Fe coordination environment in Fe(II)- and Fe(III)-silicate glasses via the Fourier-transform analysis of Fe K-XANES. Physica Scripta. Vol. T115, 215–217.
[12] Colangelo CM, Lewis LM, Cosper NJ, Scott RA. (2000) Structural evidence for a common zinc binding domain in archaeal and eukaryal transcription factor IIB proteins J Biol Inorg Chem. Apr; 5(2):276-83.
[13] Wellenreuther G, Parthasarathy V, Meyer-Klaucke W.(2010) Towards a black-box for biological EXAFS data analysis. II. Automatic BioXAS Refinement and Analysis (ABRA). J Synchrotron Radiat. Jan; 17(1):25-35.
[14] Lancaster WA, Praissman JL, Poole FL 2nd, Cvetkovic A, Menon AL, Scott JW, Jenney FE Jr, Thorgersen MP, Kalisiak E, Apon JV, Trauger SA, Siuzdak G, Tainer JA, Adams MW. (2011) A computational framework for proteome-wide pursuit and prediction of metalloproteins using ICP-MS and MS/MS data. BMC Bioinformatics. Feb 28;12:64.
[15] Shi W, Punta M, Bohon J, Sauder JM, D'Mello R, Sullivan M, Toomey J, Abel D, Lippi M, Passerini A, Frasconi P, Burley SK, Rost B, Chance MR. (2011) Characterization of metalloproteins by high-throughput X-ray absorption spectroscopy. Genome Res. Jun;21(6):898-907.